JOURNAL OF VIROLOGY, Nov. 1995, p. 7354–7361 Vol. 69, No. 11
0022-538X/95/$04.00+0

Mode of Spread to and within the Central Nervous System after Oral Infection of Neonatal Mice with the DA Strain of Theiler's Murine Encephalomyelitis Virus

YOUNG M. HA-LEE,[1]† KEITH DILLON,[1]‡ BELA KOSARAS,[2] RICHARD SIDMAN,[2] PAULA REVELL,[3] ROBERT FUJINAMI,[4] AND MARIE CHOW[1,3]*

Department of Biology, Massachusetts Institute of Technology, Cambridge, Massachusetts 02139[1]; Division of Neurogenetics, New England Regional Primate Research Center, Harvard Medical School, Southborough, Massachusetts 01772-9102[2]; Departments of Microbiology and Immunology and of Pathology, University of Arkansas for Medical Sciences, Little Rock, Arkansas 72205[3]; and Department of Neurology, University of Utah, Salt Lake City, Utah 84132[4]

Received 16 May 1995/Accepted 1 August 1995

Theiler's murine encephalomyelitis virus is a neurotropic enterovirus known to cause biphasic neural disease after intracerebral inoculation into adult mice. The present study characterizes a neonatal mouse model with a high disease incidence for the study of the acute phase of the pathogenesis of the DA strain of Theiler's murine encephalomyelitis virus after oral infection. The route of viral spread to and within the central nervous system (CNS) was determined by examining the kinetics of viral replication in various organs and by performing histopathological analysis. Viral antigen was detected widely in the neonatal CNS, mainly in the gray matter, and it was asymmetrical and multifocal in its distribution, with considerable variation in lesion distribution from animal to animal. Necrotizing lesions appeared to expand by direct extension from infected cells to their close neighbors, with a general disregard of neuroanatomical boundaries. The diencephalon showed particular susceptibility to viral infection. Other areas of the CNS, including the cerebellum and dentate gyrus of the hippocampus, were consistently spared. Neurons with axons extending peripherally to other organs or receiving direct input from the peripheral nervous system were not preferentially affected. The kinetics of viral replication in the liver, spleen, and CNS and the histopathological findings indicate that viral entry to the CNS is via a direct hematogenous route in orally infected neonatal mice and that the disease then progresses within the CNS mainly by direct extension from initial foci.

Theiler's murine encephalomyelitis virus (TMEV) is a neurotropic enterovirus which produces poliovirus-like neurological disease in natural mouse populations (10). There are two subgroups of TMEV strains (4, 6). One subgroup, which includes the GDVII and FA strains, induces a severe acute encephalitis after intracerebral (i.c.) inoculation into adult mice. Mice infected with the other subgroup, which includes the DA and BeAn strains, display an unusual biphasic disease pattern in the central nervous system (CNS) after i.c. inoculation. The early phase of infection features an acute encephalomyelitis, mainly of the CNS gray matter, which causes asymmetrical motor weakness somewhat resembling poliomyelitis. Weeks later, the surviving animals develop the second phase of TMEV disease, which is characterized by patchy demyelination in the CNS. Similarities between this model and multiple sclerosis in humans (2, 6) have served to focus interest on the later demyelinative stage of TMEV disease after i.c. infection. However, TMEV is an enteric virus (10), and to understand its pathogenesis, the disease should be evaluated after oral infection. However, per os (p.o.) inoculation usually causes asymptomatic enteric infection in adult immunocompetent mice (10). Thus, neurological signs are typically seen at such a low frequency as to render TMEV pathogenesis after p.o. inoculation difficult to study.

Previous studies of TMEV disease after i.c. inoculation had indicated that mortality rates were higher in neonatal than in adult mice (8), suggesting that neonatal mice might similarly be more susceptible to TMEV infection after p.o. inoculation. Thus, neonatal mice at different ages were inoculated with purified TMEV (DA strain) and monitored for behavorial signs suggestive of encephalitis or other neurological disease. Such general signs as lethargy, weight loss or failure to gain weight, and general failure to thrive as well as specific signs associated with neural disease, such as abnormal startle reflexes, tremulousness, and various degrees of limb paralysis, were observed in the infected mice. Mortality was highest following the inoculation of 1-day-old mice and gradually decreased as the age at the time of inoculation increased (Fig. 1). Mice inoculated at 1 and 2 days of age consistently showed signs of disease followed by death. By 3 weeks after viral infection p.o. with 10^6 PFU at postnatal day 1, 90% of the mice had died; with infection on day 2 or 3, death was delayed slightly and the incidence of deaths had fallen to 85% and 58%, respectively. Interestingly, mean survival days were almost identical, regardless of the age at the time of infection; the age at the time of infection seemed to influence only the severity of the disease and the percentage of survival. The first signs of disease were usually observed between 7 to 9 days postinoculation (p.i.), and death occurred between 12 and 19 days p.i.

All mice infected within the first 2 days after birth displayed a variety of neurological signs. Approximately 50% of the infected neonates showed paralysis of one or more limbs. The incidence of paralysis among the four limbs was similar. Mice infected at lower doses or later ages (3 to 5 days postnatal) usually showed failure to gain weight, weakness, and other nonspecific signs. Although no deaths were observed in mice infected at 5 days of age, a few of these mice did show mild signs of disease. Mice older than 7 days at the time of inoculation never showed visible signs

* Corresponding author. Phone: (501) 686-5155. Fax: (501) 686-5362.
† Present address: Laboratory of Molecular Immunology, Samsung Research Institute, Seoul, Korea.
‡ Present address: Department of Biology, Fisk University, Nashville, TN 37208.

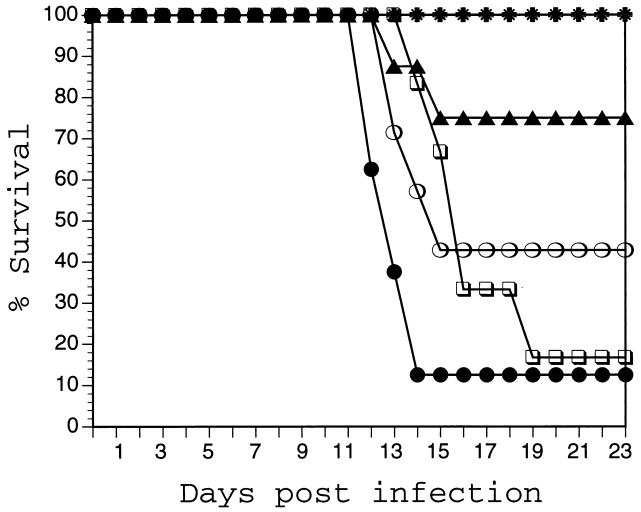

FIG. 1. Age dependence of disease incidence. Animals were infected at different ages from 1 day to 14 days of age with either 10^4 or 10^6 PFU per animal with a polyethylene catheter which was passed into the esophagus. The mice were lightly anesthetized with methoxyflurane prior to intubation. The virus was diluted in phosphate-buffered saline containing blue food dye just prior to inoculation; the blue dye allowed the virus inoculum to be visualized in the stomach through the translucent abdominal wall and thus allowed monitoring of whether the virus might have been inadvertently deposited in other regions. Only mice which were cleanly inoculated via the stomach were included in this and subsequent studies. Eight to 10 mice were used for each sample group. ●, 1-day-old mice at 10^6 PFU per animal; ○, 1-day-old mice at 10^4 PFU per animal; □, 2-day-old mice at 10^6 PFU per animal; ▲, 3-day-old mice at 10^6 PFU per animal; ∗, 5-day-old mice at 10^6 PFU per animal; ▮, 7-day-old mice at 10^6 PFU per animal; and ✣, 14-day-old mice at 10^6 PFU per animal.

of disease, and all survived. After 21 days p.i., all surviving mice, regardless of the day of inoculation, appeared to recover. Consistent with the neurological symptoms, the titers of TMEV in different tissues from infected mice were highest in the brain and spinal cord of infected animals (data not shown). Histological analyses demonstrated the presence of mononuclear cell infiltrates and perivascular cuffs and extensive neuronal destruction, consistent with meningitis and severe encephalitis (Fig. 2). In addition, immunohistochemical analysis of the diseased CNS with TMEV-specific polyclonal sera demonstrated that even before neuronal loss had become prominent and in areas where perivascular inflammation was still mild, staining for viral antigen was commonly intense in many neurons (see Fig. 4). Thus, the presence of viral titers, tissue pathology, and the distribution of viral antigen within the CNS demonstrated that the neurological signs observed in infected mice were caused by TMEV infection of the CNS.

Route of virus entry into the CNS. (i) Kinetics of viral spread after p.o. infection. The high morbidity (100%) coupled with the temporal consistency with which signs were detected suggested that the neonatal mouse provides an excellent model for the study of the route of viral spread from the gastrointestinal tract to the CNS. The kinetics of viral spread in mice inoculated p.o. on postnatal day 1 was assessed by measuring viral titers in various tissues at several time points (Fig. 3). Viral titers in the small intestine declined rapidly after inoculation and remained at low but detectable levels (Fig. 3A). Since clearance of the blue dye (which is added to the virus inoculum to observed the accuracy of the p.o. inoculation) was not complete until after 24 h p.i., it is likely that most of the viral titer detected within the first 24 h p.i. represents the initial virus inoculum and not de novo viral replication. Infectious virus in such well-vascularized tissues as the spleen and liver was detected at 8 h p.i. (Fig. 3B and C). In contrast, titers in the brain and spinal cord at 24 h after inoculation were lower than those in the spleen, liver, and blood but rose exponentially as the infection progressed (Fig. 3E and F). Although slightly higher titers were observed consistently at all time points in the rostral (cervical and thoracic) versus the caudal (lumbar and sacral) spinal cord segments of each individual animal (Fig. 3F), virus titers appeared in brain and spinal cord tissues simultaneously and the titers in all CNS tissues were similar. The absence of detectable virus in the CNS at 8 h after p.o. inoculation contrasted with the titers observed in the spleen, liver, and blood and indicated that viremia preceded infection of the CNS. This was independently confirmed by the distribution of the viral lesions within the CNS.

(ii) CNS pathology. Viremia preceding infection of the CNS raised the issue of whether CNS infection occurs by direct entry from the gastrointestinal tract via neural routes, by direct invasion of the CNS from the bloodstream, or by infection of peripheral organs, such as muscle, and subsequent entry of the virus from these secondary sites via peripheral neural routes. To explore this issue, the CNS pathology in mice inoculated p.o. on postnatal day 1 was evaluated. Random sections of brains from two infected mice at 3 days p.i. and two mice at 5 days p.i. were examined. Serial sections throughout the brains of two mice at 6 days p.i., three mice at 7 days p.i., and two mice at 8 days p.i. were examined. Similarly, serial spinal cord sections at the sacral, lumbar, thoracic, and cervical levels from the same animals and from two additional mice at 9 days p.i. were examined.

(a) Overview. No lesions or cells staining positively for viral antigen were observed in random sections of brains from mice at 3 and 5 days p.i. One of the 6-day and one of the 7-day animals showed only minimal meningeal inflammation, with no perivascular inflammation or viral antigen-positive blood-derived or endogenous CNS cells. The brains of all other mice examined histopathologically at 6 to 8 days after inoculation on postnatal day 1 showed extensive inflammation, immunohistochemical evidence of viral replication, and tissue necrosis within the CNS. In general, viral replication and antigen staining in tissues appeared to increase progressively from days 6 through 8 in the brains. Spinal cords showed viral antigen-positive neuronal cells and extensive inflammation on days 8 and 9 but not earlier.

(b) Stages of the virus-induced lesion. The types of lesions in the CNS and their times of appearance allowed us to infer a sequence of stages for the viral infection from the static histological images. After the initial histological signs of mild meningitis, the cell bodies and dendrites and some axonal processes of scattered large, medium, and small neurons (singly and in groups) stained strongly with the anti-TMEV DA capsid antibody (Fig. 4). Commonly, inflammation was minimal in the immediate vicinity of such stained neurons, though occasionally perivascular cuffs of exogenous mononuclear cells around small blood vessels and one to several virus-stained microglial cells were observed close by. As infection proceeded, perivascular cuffing with blood-derived mononuclear cells became increasingly prominent, and the positively stained neurons changed their shapes by retracting or lysing dendritic branches and rounding their cell bodies (Fig. 4C to E). These signs of neuronal infection appeared to be succeeded by the appearance of intermediate-sized lesions containing numerous virus-positive, lysed neurons; in their vicinity, the neuropil contained immunostained granular and amorphous debris, some of it in microglial cells (Fig. 4F). In particular areas of the brain that appeared most consistently and severely infected, large necrotic lesions in which virtually all CNS cell types were destroyed were observed (Fig. 2). In the center of such pannecrotic lesions, few intact immunostained cells were observed. This necrotic zone was enveloped by a zone featuring both prominent perivascular cuffing consisting of immunonegative, blood-derived mononuclear cells and a prominent reduction in the number of neurons. This inflammatory zone, in turn, was surrounded by another more or less concentric zone which was rich in microglial cells and contained a slightly reduced number

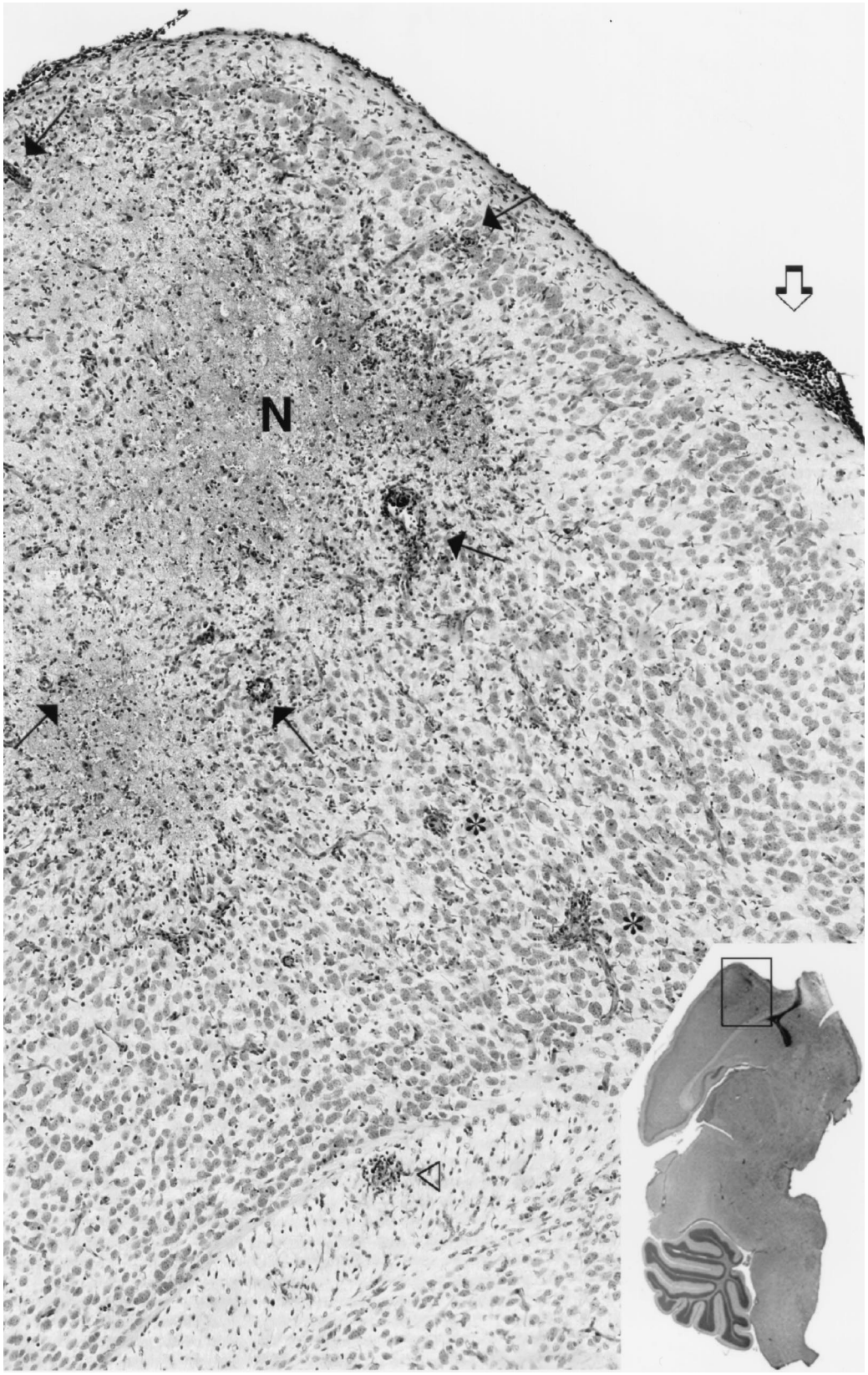
N

FIG. 2. Concentric zones of defined tissue responses around necrotic virus-induced lesions in the brain of a 2-week-old mouse infected at postnatal day 1. Tissues were fixed in cold 4% paraformaldehyde in 0.1 M phosphate buffer (pH 7.4), embedded in paraffin, serially sectioned at thicknesses of 10 μm, and stained with hematoxylin and eosin. Serial sections throughout the brain and spinal cord were examined. Overlapping fields of individual tissue sections were captured at medium magnification (×200) with a high-resolution digital camera (Leaf Systems, Southborough, Mass.) and were stored on a Macintosh Quadra 950 computer (Apple). These overlapping digitized fields were edited and assembled with standard commercial software (Adobe Photoshop; Adobe Systems) and were printed electronically with a Canon continuous-tone color printer. The inset at the lower right shows a parasagittal section through the brain, with the cerebellum at the bottom left and the frontal pole of the cerebral cortex within the rectangular box at the top. The area within the box is enlarged in the rest of the figure. The letter N lies in the center of a prominent area of almost totally necrotic eosin-stained tissue containing clusters of microglial cells around its perimeter. This zone is surrounded by a ring of tissue containing blood vessels with prominent perivascular cuffs of inflammatory cells (arrows) and markedly reduced numbers of neurons. The top two arrows have their tails in the cortical molecular layer and point to perivascular cuffs that lie in the outer compact neuronal layer of the limbic cortex. The deeper limbic cortical layers are severely disrupted. To the right, beneath the prominent inflammatory cuff around a meningeal vessel (open arrows), the orbital cortex is relatively well preserved. Ventral to (below) the necrotic area, the gray matter is diffusely strewn with microglial cells, and two of the larger perivascular cuffs in this region are marked with asterisks. An additional inflammatory focus (open triangle) is prominent in the white matter of the corpus callosum, near the bottom middle of the figure.

of neurons. At the periphery, the viral lesion gave way gradually to more normal appearing tissue. Lesions at all stages were restricted to the gray matter, except for occasional inflammatory foci in the white matter (Fig. 2). Inflammatory infiltrates in the meninges were prominent on days 7 and 8, typically in areas rich in immunopositive neurons. However, no immunohistochemical staining was observed in vascular endothelial cells, meningeal cells, or morphologically identifiable astrocytes or oligodendroglial cells. At progressively later times p.i., the trend toward larger necrotic lesions with virus-containing neurons at the lesion margins coupled with concentric zones of inflammation and virus-positive cells surrounding each necrotic virus lesion suggests that spread within the CNS is achieved by uptake of progeny virus by neighboring neurons. In addition, the viral lesions in the CNS did not follow anatomical boundaries, an indication that during spread within the CNS, the virus does not appear to be transported long distances within axons and across synapses.

(c) Anatomical distribution of lesions. Interpretation of the mode of entry into the CNS must be based on the initial distribution of the lesions within the CNS. If viral entry into the CNS were achieved solely by transport in axons which innervate peripheral tissues, one would expect to see several defining characteristics. First, the initial CNS neurons to contain DA viral antigen would be those whose axons innervate the peripheral tissues in which the DA TMEV is replicating. Second, the distribution of viral lesions within the initial CNS sites should be bilaterally symmetrical. Finally, because the patterns of neurological innervation are essentially identical from animal to animal, the pattern of viral lesions would be expected also to be invariant within the limits of the histological analysis. Thus, the distribution of CNS lesions was evaluated as the infection progressed.

Within the brain, viral lesions were restricted to the gray matter. No immunopositive oligodendrocytes or astrocytes were detected in the white matter, and the only lesions seen in white matter were occasional perivascular cuffs of mononuclear blood cells (Fig. 2). Within the gray matter, a large and coherent zone of tissue with a volume of several cubic millimeters centered on the diencephalon was affected in almost all 7- and 8-day-p.i. animals, and it was reconstructed in three dimensions from the serially sectioned brains of one 7- and one 8-day-p.i. animal. In the animal illustrated in Fig. 5, this zone extended from the junctional area between the rostral midbrain and caudal thalamus on one side of the brain, through the length of the diencephalon and septal area bilaterally, and into the cortex on the contralateral side of the forebrain. Every histological section in this zone displayed prominent perivascular inflammation, numerous immunolabelled neurons and microglial cells, and moderate necrosis.

The most advanced disease was observed in two of the three 8-day-p.i. animals; in addition to having the diencephalic lesion described above, each of these animals showed severe pathology in other parts of the cerebrum. In both of these animals, on one side only, the frontal pole of the cerebral cortex and the adjacent olfactory bulb were severely affected. In one of them,

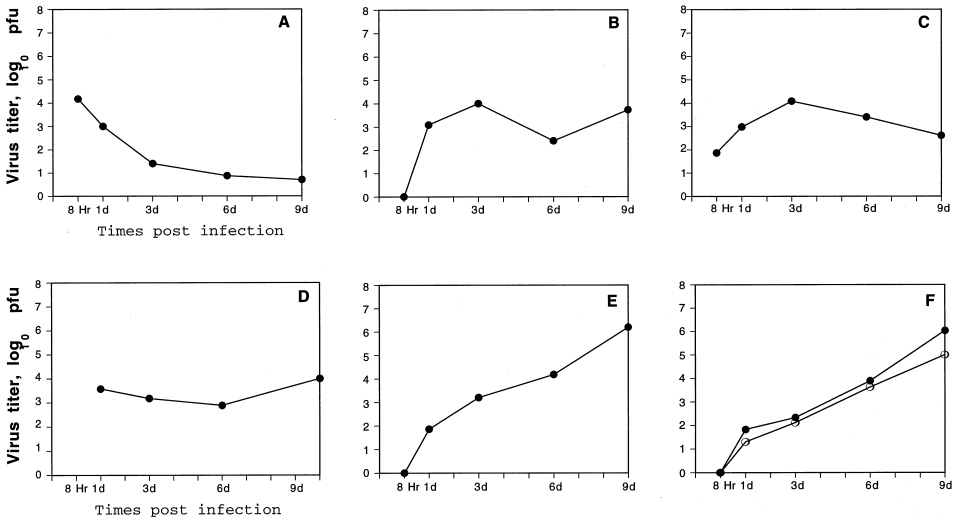

FIG. 3. Kinetics of viral spread within infected mice. One-day-old mice were inoculated p.o. with 10^6 PFU, and the viral titers present in the different organs at 1, 3, 6, and 9 days p.i. were determined by plaque assays. Each titer represents the average value for two to three infected mice; the individual titers were within 30% of each other. Titers from the small intestine (A), liver (B), spleen (C), brain (E), and spinal cord (F) are shown as PFU per 10 mg of tissue. Blood titers (D) are shown as PFU per milliliter. Spinal cord samples (F) were dissected into rostral (●) and caudal (○) regions prior to titration. The zero titers observed for the liver and brain samples at 8 h p.i. indicate that viral titers were below the detection levels of the assays. The threshold of sensitivity in the plaque assays (as determined by reconstruction experiments) was approximately 5 PFU/10 mg of tissue.

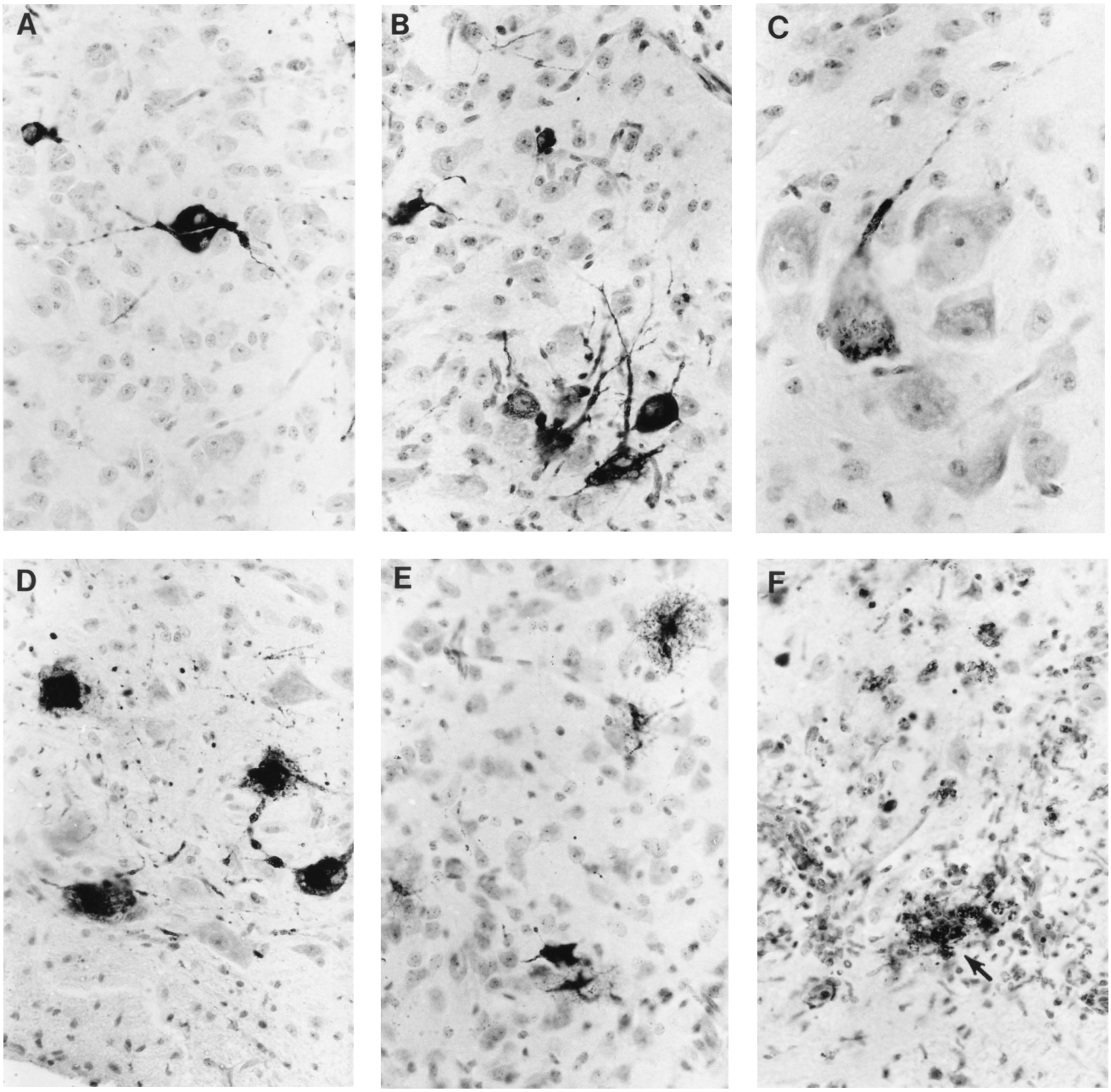

FIG. 4. Inferred stages of the virus-produced neuronal lesion, all from specimens processed at 8 days p.i. Immunohistochemical staining was carried out according to the instructions accompanying the Vectastain ABC kit (Vector Lab), with the following modifications. TMEV DA reactive polyclonal rabbit antiserum was diluted 1:500 in 1% normal goat serum (12). The anti-rabbit immunoglobulin G antibody was diluted 1:50 in 1% normal goat serum and incubated for 2 h at room temperature or overnight at 4°C. Sections were counterstained with hematoxylin (Sigma). Alternate slides were stained with hematoxylin and eosin for histopathological analysis. (A) An adjacent pair of spinal cord neuron cell bodies are immunohistochemically positive with polyclonal TMEV DA antisera, except for the unstained cell nuclei; several of their neurites also are positive. A smaller stained neuron lies in the upper left corner. This field appears at a lower magnification near the middle of Fig. 6A. (B) A cluster of four neurons with prominent dendritic processes are strongly stained. Two additional stained neurons lie among other unstained neurons of similar size in the upper part of the field. Panels A and B are sections from the spinal cord of a mouse sacrificed at 8 days p.i. (C and D) Neuron cell bodies immunostained for virus are becoming rounded, and their neurites are beaded and appear fragmented. (E) The five stained neurons appear to have lost their processes and are in various stages of lysis. (F) The remnants of a stained neuron (arrow) are being engulfed by activated microglial and macrophage cells; other microglial clusters, some immunopositive and some not, are prominent throughout the field.

the cingulate and entorhinal cortical components of the limbic system and the neocortex of the frontal and parietal regions were also affected by a series of independent foci of various sizes. In the other, the hippocampus proper and the subiculum showed moderate perivascular inflammation and had scattered immunolabelled neurons, though the adjacent dentate gyrus of the hippocampal formation was spared in this and all other animals. The medulla was affected also in an asymmetrical fashion in all animals. However, in contrast to the lesion in the thalamus and forebrain regions of the same individual mice being continuous, the sites of inflammation and neuronal labelling were characteristically small and scattered (data not shown). They varied in number and position from animal to animal and even from section to section in a given animal. The pons was relatively spared in all animals, and the cerebellum was entirely negative. Thus, viral replication sites as indicated immunohistochemically are not

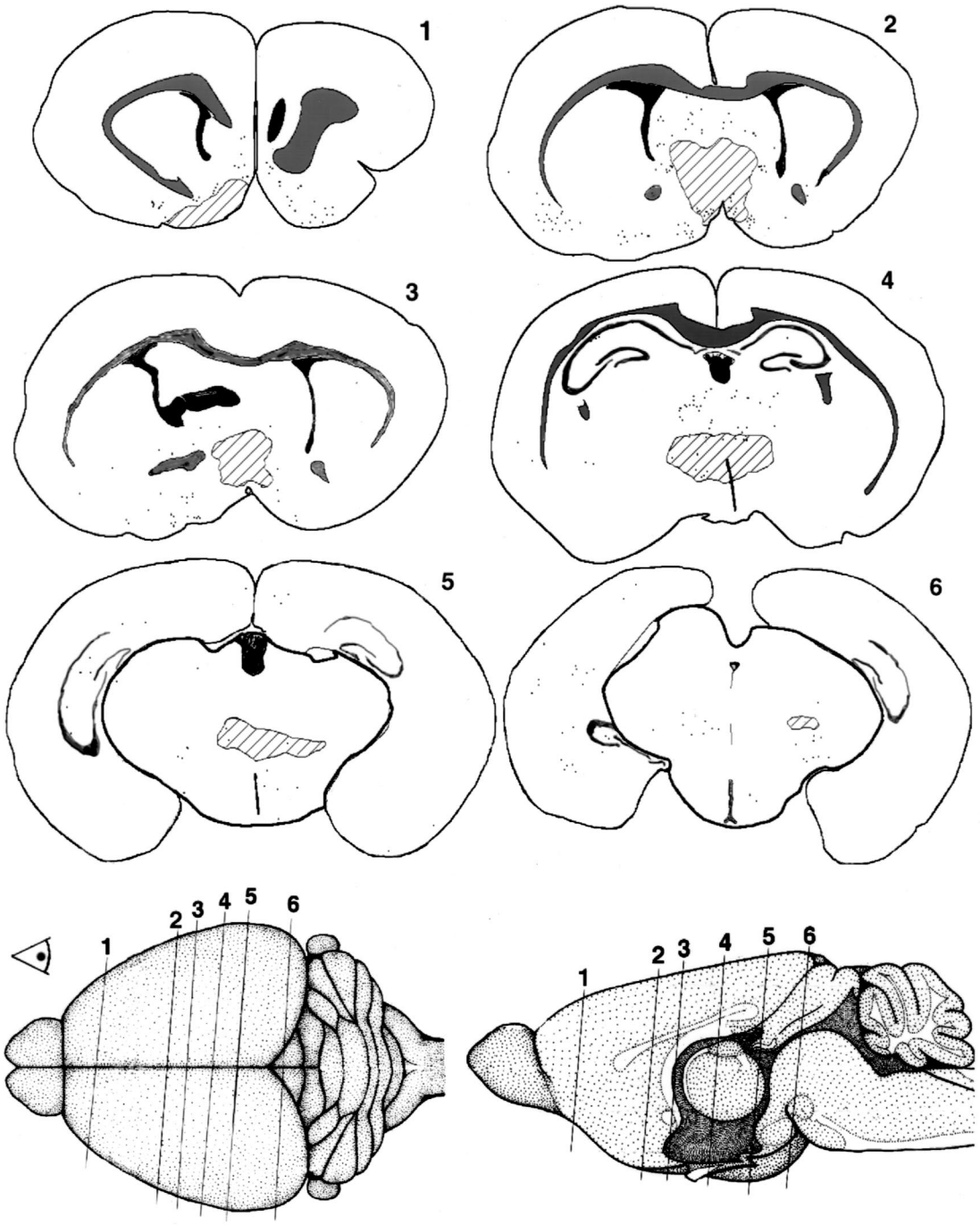

FIG. 5. Three-dimensional distribution of virus lesions in the brain of a mouse at 8 days p.i. Adobe Photoshop software was used to trace the anatomical boundaries on representative digitalized images from a complete set of serial sections of a mouse brain at 8 days p.i. The tracings diagram a coherent zone of intense inflammation and tissue necrosis (diagonal shading) that extends continuously from the medial aspect of the base of the forebrain on the right side (section 1, left side of the illustration) through the septal area bilaterally (section 2), the preoptic part of the hypothalamus (section 3), the ventral thalamus (sections 4 and 5), and the left side of the midbrain (section 6, right side of the illustration). This zone of inflammation and necrosis did not extend into the olfactory bulbs rostral to section 1 (not shown) or into the more dorsal parts of the midbrain (section 6) or the pons caudal to section 6 (not shown). The small dots on sections 1 to 6 each represent an immunolabelled neuron. Their positions are, for the most part, outside the area of intense inflammation and necrosis, and they probably represent milder or more recent sites of viral infection. For purposes of anatomical orientation in sections 1 to 6, the white matter of the corpus callosum is shown in gray on sections 1 to 4, the white matter of the anterior commissure is shown in the same shade of gray to the left and right of the centrally positioned inflammatory lesion in sections 2 and 3, the vertical slit-like profiles of the lateral ventricles are shown in black in sections 1 to 3, the third ventricle is shown in black in section 3 (on the right side of the brain [left side of the illustration], just medial to the vertical lateral ventricle) and in the midline in sections 4 and 5, and the triangular profile of the small aqueduct of Sylvius in the dorsal midline part of the midbrain is shown in section 6. The tightly curved, open-ended dentate gyrus interlocked with the larger curving profile of the hippocampus appears bilaterally in gray just beneath the corpus callosum in section 4 and appears progressively more ventrally positioned in sections 5 and 6. The varying positions and sizes of the hippocampus and other structures on the two sides of a given section result from the oblique angle of the sectioning of this particular brain specimen, as illustrated by lines 1 to 6 (corresponding to the planes of sections 1 to 6) on the dorsal view of the mouse brain at the bottom left and on the midsagittal view at the bottom right. (These two drawings of adult mouse brains are modified from Sidman et al. [9].) A given section passes through the right side of the brain more caudally than through the left side and through the dorsal aspect of the brain more caudally than through the ventral aspect. Thus, for example, section 3 just catches the rostral part of the third ventricle in the right side of the brain (left side of the section 3 illustration) but passes rostral to the third ventricle in the left side of the same section. As the symbolic eye just above the olfactory bulbs on the bottom left illustration is meant to suggest, the viewer is in front of the brain, so the left side of the drawing of any given section shows the right side of the brain.

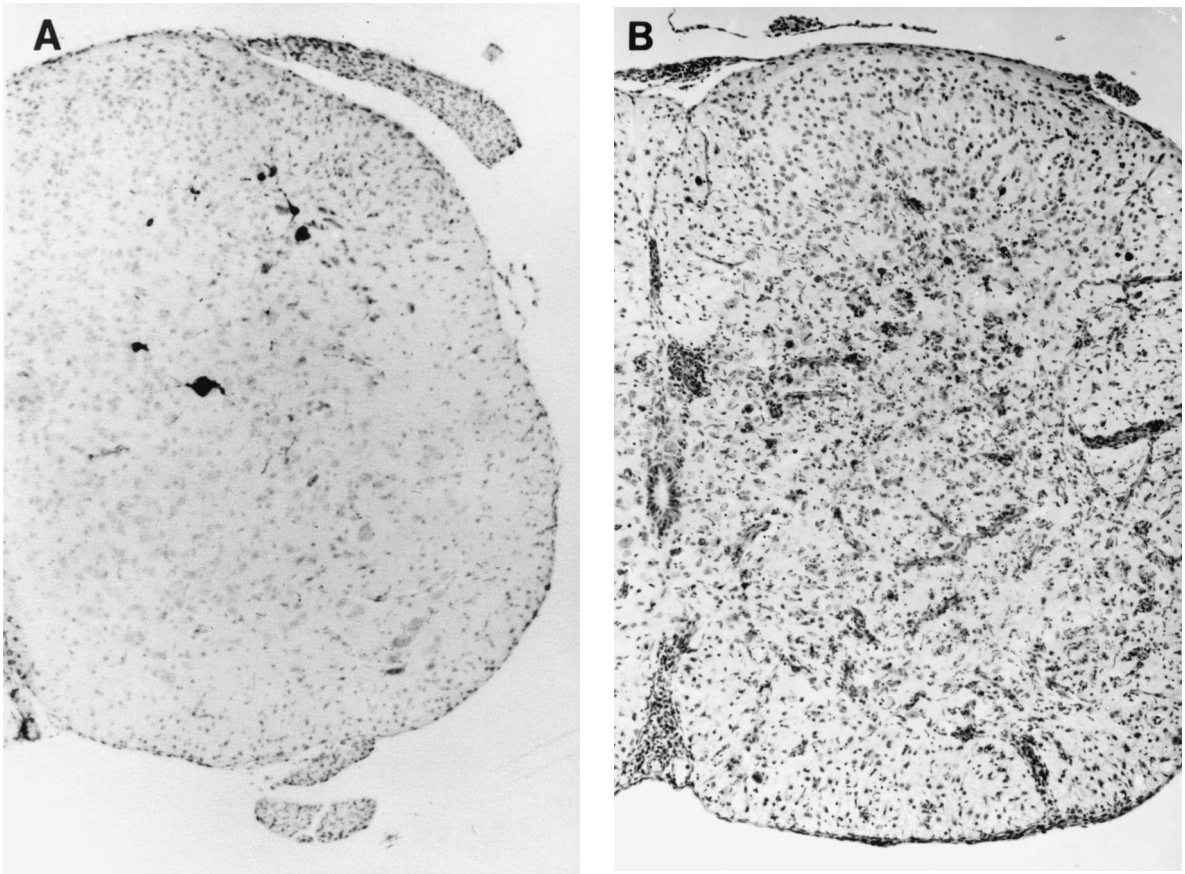

FIG. 6. Viral lesions in the spinal cord. (A) Several virus-stained neurons are seen in the dorsal horn of the spinal cord (top half of illustration), and almost none are seen in the ventral horn (bottom half of illustration). The pair of stained cells near the middle of the figure are the same ones illustrated at higher magnification in Fig. 4A. This section was taken from a mouse at 8 days p.i. (B) This spinal cord, at 9 days p.i., displays intense inflammation at all levels. Neuronal destruction is very advanced, and microglial clusters are prominent at sites formerly occupied by neuronal cell bodies. No immunopositive neurons remain.

entirely random; some regions (e.g., the cerebellum and dentate gyrus of the hippocampal formation) were never infected, while other regions (e.g., the diencephalon and medulla and almost all segments of spinal cord) were infected in the majority of animals. However, these regions of susceptibility do not directly innervate peripheral tissues and contain neurons that synapse with other neurons in the unaffected areas of the CNS.

In the spinal cords of the mice examined at 8 and 9 days p.i., the areas of inflammation were again randomly distributed on the left and right sides and at the ventral, intermediate, and dorsal levels in almost all cervical, thoracic, lumbar, and sacral segments (Fig. 6A). Patches of inflammation within the spinal cord were small but numerous and, as in the brain, were typically enveloped by immunostained neurons and microglial cells. The lesions showed no particular predilection for anatomically defined compartments (such as the ventral horn, with its rich complement of motor neurons) and no symmetry between the left and right sides. At the most advanced stage, these smaller lesions appear to merge to involve the entire gray matter within a given cross section (Fig. 6B). At these stages, extensive neuronal necrosis and prominent microglial nodules indicative of neuronophagia became prominent (Fig. 6B). Despite this prominence of microglial cells in affected areas, relatively few of these cells were immunopositive. However, in advanced lesions, there was considerable immunohistochemical staining which was not localized to cell bodies but might represent either viral antigen in extracellular space or in microgial cell processes which were not resolvable in the tissue sections.

In sum, the CNS pathology observed in both the brain and spinal cord sections presents several general characteristics. Virus-containing neurons are distributed preponderantly in areas of the CNS that are not directly connected via axons to peripheral tissues. The distribution of lesions and immunolabelled cells is asymmetrical. Viral antigen is not confined to anatomically defined boundaries within a given brain. Finally, the patterns of viral lesions vary among mice. The neuroanatomical data in aggregate are most consistent with the view that TMEV DA enters the CNS stochastically via a hematogenous route rather than via defined neural pathways from infected peripheral tissues. The kinetic analysis demonstrating that viremia precedes CNS infection (Fig. 3) further supports the interpretation that the route of entry is hematogeneous.

Mode of entry into the CNS and spread within the CNS. After p.o. inoculation, TMEV DA virus could theoretically enter the CNS via any or all of several possible neurological routes.

(i) Because of inadvertant introduction into the nasal cavity during p.o. inoculation and direct contact with the olfactory epithelium, the virus might pass along axons of the olfactory nerve and thus gain access to the olfactory bulb of the brain. The distribution of CNS lesions indicates that this model is unlikely. In animals in which olfactory bulb involvement was seen, the sites of viral antigen varied from animal to animal, were not affected in advance of other CNS regions, and were not in the regions of the bulb where olfactory nerve axons make synaptic contacts with CNS target neurons.

(ii) The virus might be carried from the gastrointestinal tract to the CNS via motor and/or sensory axons of the vagus nerve. These axons innervate the gastrointestinal tract from the esoph-

agus to beyond the small intestine. The motor axons emerge from parent neuronal cell bodies in the dorsal motor nucleus of the vagus in the medulla of the brain and synapse on neurons in the intestinal wall; the sensory axons emerge from cell bodies in the nodose ganglion and synapse on second-order target neurons in the nucleus of the tractus solitarius of the medulla. If this mode of CNS entry were operant, the first CNS neurons to contain DA viral antigen, even in the presence of viremia, would be these well-characterized neurons in the vagus-solitarius complex of the medulla. This was the pattern observed in neonatal mice inoculated p.o. with reovirus type 3 Dearing, clone 9 (7). However, no such pattern of antigen staining was observed in the present study. Thus, the DA strain of TMEV appears not to be transported directly from the gut to the CNS via the vagal complex.

(iii) Virus might seed from the bloodstream to other peripheral tissues and then reach the CNS via retrograde transport in axons which innervate those particular tissues. This model would predict that the first CNS neurons to contain virus would be the somatic motor and sympathetic and parasympathetic neurons or secondary sensory neurons of the spinal cord and brainstem which directly innervate the peripheral sites of viral replication. In TMEV-infected newborns, these neurons, readily recognized in histological sections, were not preferentially or even consistently involved at early times after infection. However, because virus-positive primary motor neuron cell bodies in the spinal cord and brainstem are seen at later stages of disease after p.o. infection, it is impossible presently to determine whether these regions were seeded via retrograde intraaxonal spread from infected skeletal muscle or, like the nonmotor regions in the brain and spinal cord, were variably seeded from the bloodstream. We favor the latter as the major process because of the variable involvement among spinal cord segments, the variations between the left and right sides, and the lack of predilection for motor versus nonmotor neurons in the affected regions.

The distribution of lesions and of immunohistochemically positive cells is also inconsistent with the idea that the virus might be transported within the CNS along cerebrospinal fluid pathways. Ependymal cells lining the ventricles were consistently spared. The prominent germinal zone immediately outside the ependyma of the lateral ventricles of the neonatal mouse brain was likewise spared (Fig. 2), and in general, the periventricular gray matter throughout the CNS was not a prominent site of immunochemically positive cells or of lesions.

The distribution of viral antigen within the CNS is inconsistent with neurological routes of entry and consistent with entry directly from the bloodstream. Meningitis and perivascular cuffing with blood-derived cells are characteristic early features in the brains of these infected mice. In addition, most of the TMEV-affected neurons have axons that are entirely confined within the CNS and therefore could not have received virus directly from peripheral tissues via axonal transport mechanisms. The multifocal nature and widespread distribution of the initial lesions and the variability in the number and distribution of the lesions from animal to animal are also consistent with a stochastic mode of entry from the broadly pervasive vasculature of the CNS.

Although our results indicate that the virus passes into the CNS directly from the blood, the mechanism of passage is unknown. Virus particles might enter vascular endothelial cells (12) and then disseminate through the CNS. Meningitis and perivascular cuffing were prominent, indicating an immune response to the presence of virus. Although in a rare instance a viral antigen-positive, blood-derived mononuclear cell was observed in the meninges, viral antigen was not detected in the meningeal cells themselves or in vascular endothelial cells. It is possible that the immunohistochemical techniques were insufficiently sensitive to detect low concentrations of viral antigen in these cells. However, it is at least equally likely that TMEV may cross the vessel wall without replicating extensively in the endothelial cells or in the astrocytic end feet that envelop CNS capillaries. The blood-brain barrier is known to be relatively inefficient in neonatal mice (5) and might allow the passage of virus into the CNS more effectively in our neonatal model than in the previously studied adults.

The distribution of viral lesions described here has some features in common with as well as significant differences from the general pattern previously reported to occur after i.c. inoculation of neonates (8). Just as in the earlier study, lesions were consistently observed in the thalamus, brain stem, and spinal cord while no lesions were observed in the cerebellar cortex and dentate gyrus of the hippocampal formation. However, the expected lesions in the cerebral cortex, basal ganglia, and cerebellar nuclei were observed only occasionally in p.o.-inoculated mice. Within the spinal cord after neonatal p.o. infection, the involvement of nonmotor neurons appeared to be at least as frequent as that of the motor neurons of the ventral horn. The major involvement of nonlimbic components observed in the p.o.-infected newborns is also distinctly different from that reported after i.c. inoculation of adults, in which viral spread within the CNS was suggested to be through neural pathways, with a special predilection for various components of the limbic system (3, 11). Since the portal of entry strongly influences the distribution of lesions in the brain (1), differences in the distribution of lesions after p.o. or i.c. inoculations are not surprising. In addition, different regions within the CNS may display differing susceptibilities to viral infection, leading to the observed distribution of viral antigen. These differential susceptibilities in the newborn CNS may reflect differences in receptor expression and/or receptor densities on neuronal cell surfaces or utilization of different receptor molecules by the virus in different regions of the CNS. However, while differences might have been anticipated, the patterns of viral antigen distribution which were actually observed within the newborn CNS after p.o. inoculation were not predictable from the previous studies with i.c.-inoculated neonates and adult animals.

We thank B. N. Fields, M. A. Mann, A. Georgi, and H. Virgin for helpful advice and discussions.

This work was supported by program project grant P50 NS16998 from the National Institute of Neurological and Communicative Disorders and Stroke.

REFERENCES

1. **Bodian, D.** 1955. Viremia, invasiveness, and the influence of injections. Ann. N. Y. Acad. Sci. **61:**877–882.
2. **Dal Canto, M. C., and H. L. Lipton.** 1977. Multiple sclerosis: animal model of human disease. Theiler's virus infection in mice. Am. J. Pathol. **88:**497–500.
3. **Dal Canto, M. C., and H. L. Lipton.** 1982. Ultrastructural immunohistochemical localization of virus in acute and chronic demyelinating Theiler's virus infection. Am. J. Pathol. **106:**20–29.
4. **Downs, W. G.** 1982. Mouse encephalomyelitis virus, p. 341–352. *In* H. L. Foster, J. D. Small, and J. G. Fox (ed.), The mouse in biomedical research. Academic Press, New York.
5. **Johanson, C. E.** 1989. Ontogeny and phylogeny of the blood-brain barrier, p. 101–129. *In* E. Neuwelt (ed.), Implications of the blood-brain barrier and its manipulation, vol 1. Basic science aspects. Plenum Press, New York.
6. **Lipton, H. L.** 1975. Theiler's virus infection in mice: an unusual biphasic disease process leading to demyelination. Infect. Immun. **11:**1147–1155.
7. **Morrison, L. A., R. L. Sidman, and B. N. Fields.** 1991. Direct spread of reovirus from the intestinal lumen to the central nervous system through vagal autonomic nerve fibers. Proc. Natl. Acad. Sci. USA **88:**3852–3856.
8. **Rodriguez, M., J. L. Leibowitz, H. C. Powell, and P. W. Lampert.** 1983. Neonatal infection with the Daniels strain of Theiler's murine encephalomyelitis virus. Lab. Invest. **49:**672–679.
9. **Sidman, R., J. B. Angevine, and E. Taber Pierce.** 1971. Atlas of the mouse brain and spinal cord. Harvard University Press, Cambridge, Mass.
10. **Theiler, M.** 1937. Spontaneous encephalomyelitis of mice, a new virus disease. J. Exp. Med. **55:**705–719.
11. **Wada, Y., and R. S. Fujinami.** 1993. Viral infection and dissemination through the olfactory pathway and the limbic system by Theiler's virus. Am. J. Pathol. **143:**221–229.
12. **Zurbriggen, A., and R. S. Fujinami.** 1988. Theiler's virus infection in nude mice: viral RNA in vascular endothelial cells. J. Virol. **62:**3589–3596.